Laboratory and Field Test and Distinct Element Analysis of Dry Granular flows and segregation process

Cheng Yung Ming[1,3], Fung Wing Hong Ivan[2], Li Liang[3] and Li Na[1]

Department of Civil and Environmental Engineering, The Hong Kong Polytechnic University, Hong Kong[1]

Department of Architecture and Civil Engineering, City University of Hong Kong[2]

School of Civil Engineering, Qingdao University of Technology[3]

Abstract

Natural as well as fill slopes are commonly found in Hong Kong, China and many other countries, and slope failures with the subsequent debris flows have caused serious loss of lives and properties in the past till now. There are various processes and features associated with debris flow for which the engineers need to know so as to design for the precautionary measures. In this study, experiments on flume tests, friction tests, deposition tests, rebound tests have been carried out for different sizes of balls to determine the parameters required for modelling of debris flow tests. Different materials and sizes of balls are used in the flume tests, and various flow pattern and segregation phenomenon are noticed in the tests. Distinct element (DEM) debris flow modeling are also carried out to model the flow process. It is found that for simple cases, the flow process can be modelled reasonably well by DEM which is crucial for engineers to determine the pattern and impact of the debris flow. The single material and multiple material laboratory tests and numerical simulations can provide further insight into the debris flow process for which only limited field test data can be obtained in general. From the laboratory tests, large scale field tests and numerical simulations, it is also found that the particle size will be the most critical factor in the segregation process during debris flow. It is also found from the laboratory tests and numerical simulations that a jump in the flume can help to reduce the final velocity of the debris flow which is useful for practical purposes.

Keywords: flume test, field test, balls, debris flow, distinct element, flow process

1- Introduction

The terrain of Hong Kong is hilly. Many slopes (fill, cut and natural slopes) and roads are formed to cope with the rapid development of Hong Kong, China and many other developed cities. Hong Kong has a high rainfall, with an annual average of 2300mm which falls mostly in summer between May and September. The stability of man-made and natural slopes is of major concern to the Government and the public. Landslides and subsequent debris flows have caused loss of life

36 and significant amount of property damage in the past. In Hong Kong, for the 50 years after 1947,
37 and more than 470 people died due to slope failures and debris flow associated with man-made cut
38 slopes, fill slopes and retaining walls.

39 There are many reported serious slope failures and debris flow problems in China in the recent ten
40 years, due to the significant amount of constructions and inadequate stabilization to many
41 temporary or permanent fill or natural slopes. The destructive power of large scale debris flow is
42 well known, and the prevention of slope instability, reduction of debris flow destructive power by
43 the use of rigid, flexible barrier or other means are well practiced in many countries. There are
44 many cases where the slopes fail with subsequent debris flows in Hong Kong and China (Scott
45 and Wang 1997), which have created various serious problems. Based on a conservative estimate,
46 over 60 countries in the world have faced the problems of debris flow over the years. With
47 reference to Fig.1, the debris flows in Hong Kong and China have created traffic problems, loss of
48 lives and properties, and currently there are many active research works in the area of debris flow
49 in Hong Kong and China. The research works include three-dimensional slope stability analysis,
50 debris flow process, impact loads on flexible and rigid barriers and others. An example on three-
51 dimensional Morgenstern-Price slope stability analysis using 16000 columns has been carried out
52 by Cheng in 2016/2017 which is shown in Fig.2 (Lo et. al. 2018). The analysis of the non-spherical
53 surface is achieved by the use of Nurbs function as discussed by Cheng et al. (2005), and Nurbs
54 representation is a popular method as adopted in many 3D cad programs. Upon the determination
55 of the critical failure mass, and the flow path of the soil can be estimated from a distinct element
56 analysis using the method as discussed by Cheng et al. (2015). The slope failure and the subsequent
57 debris flow as shown in Fig.2 is finally protected by the use of three levels of flexible barrier
58 against the future potential debris flow.

59

61   (a)   (b)

62 Fig.1 Representative debris flow in Hong Kong and Shenzhen, China (a) Tsing Shan debris flow
63 in 1990 (King 2013); (b) debris flow in Shenzhen 2015 (see Wikipedia).

64
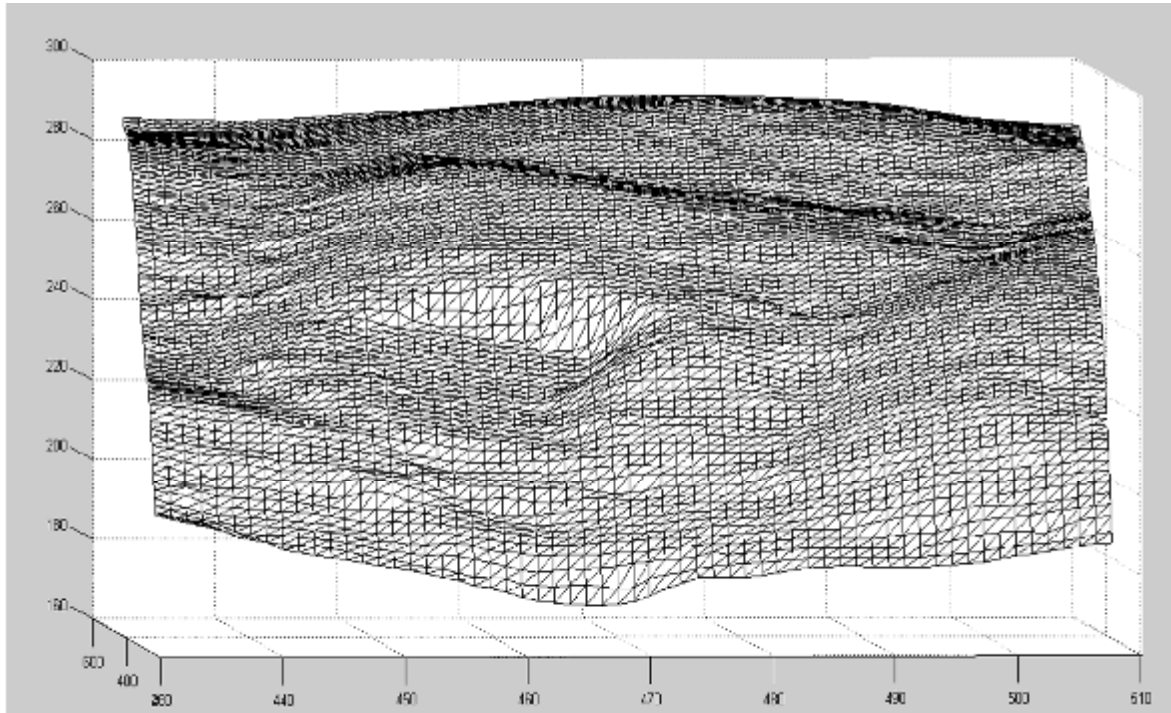
Fig.2 A three-dimensional slope stability analysis for a slope in Hong Kong by Cheng (the triangulation represent the geometry as defined by the GIS information)

Debris flow has some fundamental difficulties in the physical tests as well as numerical analysis. In general, various particles sizes will be present in a flow, and the debris mix is usually far from uniform in composition. For physical tests, it is difficulty to apply a representative debris flow mix, and the flow process is further complicated by the presence of water. For numerical simulation, it is virtually impossible to accommodate too much particles in a model, ranging from a very small particle size to cobbles or even boulder in the extreme range. Even if such a numerical model can be established, there will be serious numerical problems if the particles sizes differ too much in the system. Debris flow can be induced from gravity, driven by fluid dynamic or from both factors. The classification of debris has been given by Varnes (1978), and later modified by Furuya (1980), Ohyagi (1985), Pierson and Costa (1987), Coussot and Meunia (1996), Cruden and Varnes (1996), Hungr et al. (2001), Takahashi (2001, 2006) and others. A detailed theoretical treatment of dry granular debris flow similar to some of the single material tests in the present study has been given by Takahashi (2014) and will not be repeated here. In this study, we will concentrate mainly on the action of gravity, while the effects of water is under study by the authors.

Many scientists have carried out debris flow analysis. Lo (2004) has compare the different composition of debris flow in landsides in Hong Kong and examine the coarse and fine particle concentration. Hutter et al. (2005) has considered the flow envelops and the deposition of the debris flow. In year 1991, the U.S. Geological Survey has made a large scale flume for detailed

86 experimental tests on debris flows. Mizuyama and Uehara (1983) have made a flume which is 20
87 cm wide and 25m long, and the slope angle ranges from 5 degree to 25 degree. Liu (1996) has
88 made a 18 cm depth, 16 cm width and 150 cm length flume in Yunnan, China, and the flume
89 inclination can be adjusted from 10 to 34 degrees. Lin (2009) has made a 20 cm width 8m length
90 flume with a 2.2 m width 3 m length catchment. There are also various flume tests that have been
91 carried out by various researchers in Hong Kong and many other countries.

92 During the transportation period, segregation occurs when debris starts to flow. Iverson (1997)
93 studied the factors that influence the segregation process. He found that particle size has a great
94 effect on the segregation process, and debris with larger particle size move upward while fine
95 particles go downwards. This phenomenon is the opposite of "normal grading" in which the finer
96 particles are found at the upper layers in the lake or river and large particles rest at the bottom. The
97 main reason for the segregation is kinetic sieving, and finer particle can go through the gaps
98 between particles more easily than the larger particle. Large particles can also be found at the front
99 of the flow because of the relatively high velocity of the larger particles at the upper layer,
100 compared with the finer particles with lower velocity at the lower layer. When a stable contact
101 network for large particle is formed at the free surface, the segregation cease to occur and the balls
102 finally deposit at the catchment area.

103 For distinct element modeling (DEM) of debris flow, Jiang et al. (2003) has studied the methods
104 of generations of ball in PFC2D (Cundall 1971, 1988, Cundall and Hart 1992, Cundall and Strack
105 1979), namely the expansion method and isotropic compression method. Zohdi (2007), Halsey and
106 Mahta (2002) have discussed about the physics of granular flow; the contact model and the limit
107 of the friction coefficient. Sullivan (2011) has also compared between the theory and computation
108 in distinct element analysis. It is well known that the use of DEM can only provide qualitatively
109 instead of quantitative study up to the present (see also the discussion part).

110 In the present study, basic dry granular flow experiments will be conducted under different
111 conditions using glass and rubber balls for a basic study on the flow process and segregation. Both
112 glass and rubber balls of different diameters have been used in the tests, and combination of
113 different size and materials have also been tried in the tests for the illustration of the segregation
114 problem. The experimental results are also analyzed by distinct element analysis using program
115 PFC2D. It is true that three-dimensional distinct element modelling can be a better tool for the
116 present problems, but the previous experience in three-dimensional distinct element modelling by
117 the authors suggest that the amount of computer time can be significant. For the present study, the
118 flume in both the laboratory and field tests are relatively narrow, and off-track movement of the
119 balls/grains are not major. In view of that, two-dimensional modelling has been adopted in the
120 present study, and good results are actually obtained. The tests are performed at relatively simple
121 condition so that the basic problem of flow and segregation can be studied easily. It should also be
122 mentioned that more than 10 ten thousands photos are taken from the laboratory and field tests,
123 and such amount of information cannot be fed into a paper. In views of that, only representative

124 intermediate photos which are used for illustration are given in the present paper, while some of
125 the observed phenomena are simply described without the support of the photos.

126

127 **2. Physical flume modeling of debris flow**

128 **2.1 Instrumentation and Test Material**

129 To enhance the knowledge on the debris flow mechanism, many laboratory and large scale field
130 tests have been carried out by the authors. The laboratory model is about 1.5m long and 1.3m high
131 (adjustable). The flume in the laboratory is made of polystyrene and is designed to be flexible, and
132 the angle of inclination can be adjusted if necessary. The flume model is 40cm depth, 40 cm width,
133 140 cm length of upper flume and 100 cm for the lower flume with a 60 x 60 catchment area at
134 the bottom. Fig. 3 and Fig 4 show the schematic design of flume and flume model in the laboratory
135 tests. In order to record the motion of the particles, two high speed cameras are adopted. The first
136 one is mounted on the upper flume and the second one is fixed to the bottom flume. In the
137 laboratory tests, different sizes of glass beads and rubber beads are used to replace the use of sand,
138 and this simplification can help to assess the effects of shape and material on the segregation
139 process. In the large scale field test, real sand is used. For the material parameters, the dynamic
140 friction angle is measured by using tilting test (Pudasaini & Hutter (2007), Mancarella & Hungr
141 (2010)). The property of the glass and rubber beads are determined experimentally, and the details
142 are given in Table 1.
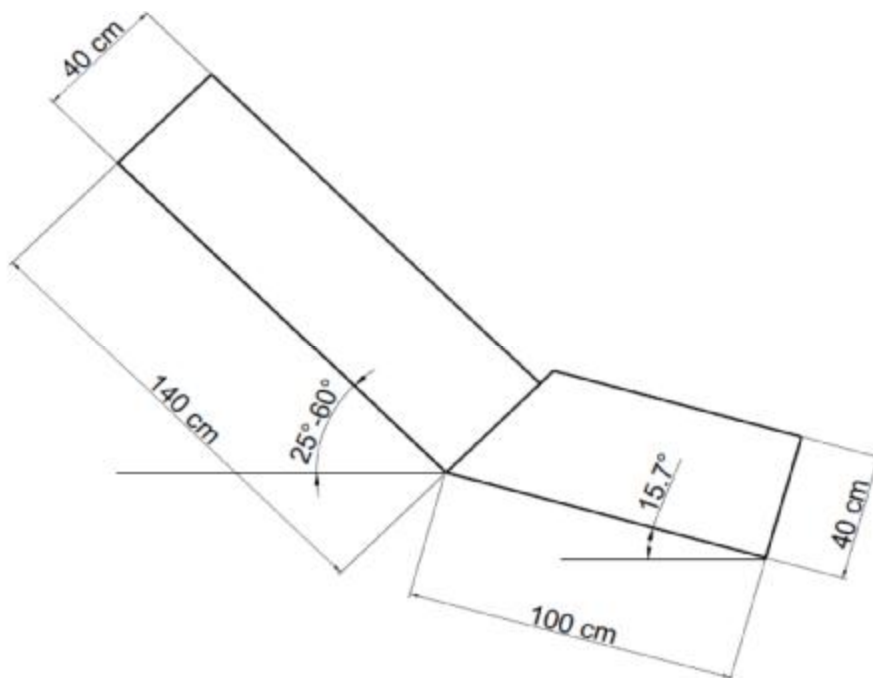
143

144   Fig.3 Schematic Design of Flume

145
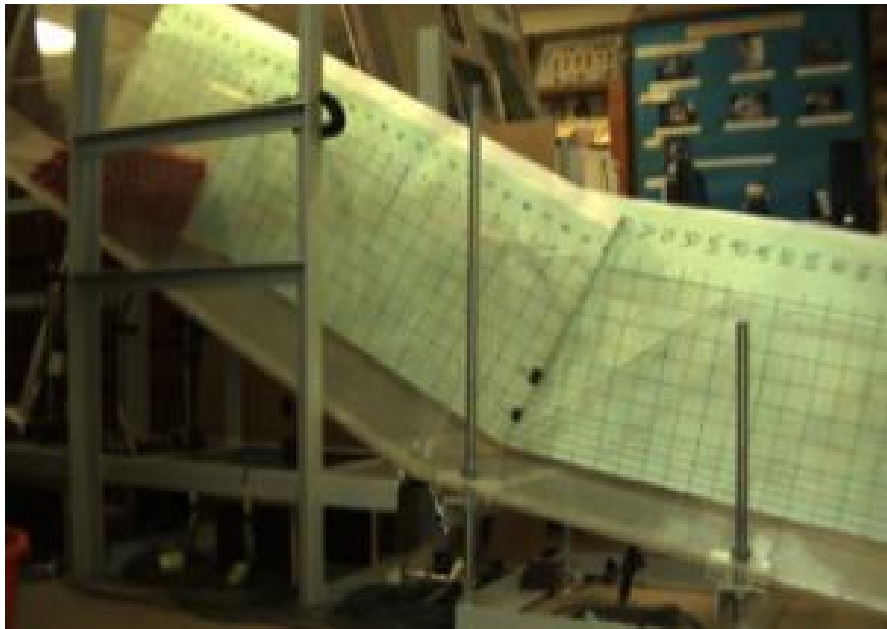
146

147   Fig.4 Flume model in laboratory
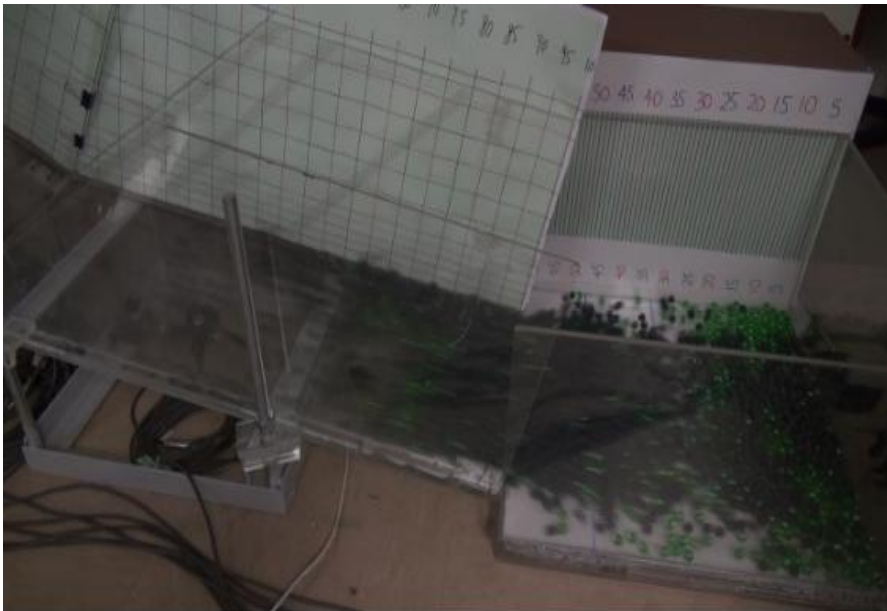
148

149   Fig 5. Flume model with a small jump in laboratory

150

151   Fig.6a Transparent glass   Fig.6b Blue glass ball

152

153   Fig.6c Green glass ball   Fig.6d White plastic ball

154

155   Fig.6e Red plastic ball   Fig.6f Black plastic ball

156

157   Table 1. The properties for the glass balls and plastic balls in laboratory debris flow test

Plastic	D(mm)	Average Weight	Density (kg/ m³)	External Friction Coefficient	Internal Friction Coefficient
White	50	105.35	1609.64	0.781	0.547
Red	30	23.382	1653.97	0.630	0.429
Black	15	2.862	1619.56	0.222	0.365
Glass	D(mm)	Average Weight	Density (kg/ m³)	External Friction Coefficient	Internal Friction Coefficient
Transparent	40	78.686	2348.11	0.102	/
Blue	25	21.121	2581.64	0.053	/
Green	16	5.744	2678.28	0.104	/

158

2.2 Test Programme

160 In the present study, the angle of the flume in laboratory is kept to be 45 degree. The effect of the
161 slope inclination will hence not be investigated in this study (to be covered by another paper later).
162 Totally 68 laboratory tests have been carried out. The 68 tests are divided into two groups: the first
163 group of tests were conducted on the flume with a small jump, and the other group of tests were
164 carried out on the flume without a jump. Such a jump is also commonly adopted in Hong Kong,
165 and this helps to lower the velocity of the debris (for small scale flow). Fig 5 shows the flume in
166 laboratory with a small jump. The effects of the particle size and the flowing mass are also studied
167 through the use of balls with different diameter, mass and combination of different balls. Table 2
168 shows only some of the test programme. Test 1 to test 48 belong to the first tests group with a
169 small flume jump. Test 1 to test 6 were carried out by using six different kinds of balls separately
170 with the same mass of 10 kg. The mass of the balls is then changed to 13.55kg and the above tests
171 are repeated again (for test 7 to 10). In order to study the segregation process for test 11 to 40, two
172 kinds of balls with different diameters were combined together, and for the same purpose in test
173 40 to test 48, three kinds of balls were combined together. Test 49 to test 68 belong to the group
174 without a small flume jump. Same as the first group of tests with a small flume jump, test 49 to
175 test 55 were carried out for same material but different sizes of balls. In test 56 to test 63,

176 combinations of two kinds of balls were tried. The last five tests were the combination of three
177 kinds of balls.

178

179   Table 2. Test Programme

Flume with a small jump			
One kind of balls	Test Number	Flow Mass	Balls
	1	10 Kg	G(Transparent)
	2	10 Kg	P(White)
	7	13.55Kg	G(Green)
	8	13.55Kg	P(Red)
Two kinds of balls	Test Number	Top Layer	Bottom Layer
	11	P(White)	P(Red)
	26	G(Trans)	P(White)
Three kinds of balls	Test Number	Top Layer	Middle Layer	Bottom Layer
	41	P(White)	P(Red)	P(Black)
	45	G(Trans)	P(Red)	P(Black)

180

Flume without a small jump			
One kind of balls	Test Number	Flow Mass	Balls
	49	10 Kg	G(Transparent)
	50	10 Kg	G(Blue)
Two kinds of balls	Test Number	Top Layer	Bottom Layer
	55	P(White)	P(Black)
	56	G(Trans)	P(Black)
Three kinds of balls	Test Number	Top Layer	Middle Layer	Bottom Layer
	67	G(Trans)	P(Red)	P(Black)
	68	G(Trans)	P(Red)	G(Green)

181   P: P refers to plastic balls, G: G refers to glass beads

182

2.3 Test procedure and test results

184 Test materials with different particle size combinations (single type of balls to multiple types of
185 balls) were put into the container which is on the top of the flume. Figure 7 shows the flow pattern
186 of single type dry granular material flowing along the flume. The video captured by high speed
187 camera can show this process clearly. When the gate of the container was pulled up, the front part
188 of flow mass become loose and start to flow along the upper flume under the action of gravity,
189 while the latter part of flow mass followed behind. Flow mass elongated when it moved forward,

190 and the shape of flow front is wedge-like type. At the moment when the particles reached the
191 bottom of the flume, the velocity direction of the balls changed because of the angle difference
192 between the upper flume and the lower flume. During the transportation period, a large amount of
193 potential energy of the initial flow mass was transferred to momentum energy accompanying by
194 energy dissipation through the grain collision and friction. Particles at the front of the flow
195 reflected back when they impacted on the wall of deposition zone and collided with the subsequent
196 particles immediately, which consumed the residual momentum energy of flow particles. Finally
197 all the particles rested in the deposition zone.

198 In reality, there are sediments and water in a debris flow. The effect of water is complicated, and
199 will not be studied in the present work. The grain size distribution is usually not uniform as in the
200 present laboratory tests. Consequently, a good understanding of the particle flow under a mixture
201 of ball sizes is important. Particle size is a vital parameter for the good understanding of multi-size
202 particle flow because it not only has an effect on the flow dynamic, but also influence the energy
203 attenuation during the whole flow process. What's more, the tilting test that is mentioned above
204 demonstrates that the dynamic friction angle depends on the particle size, specifically, larger
205 particle size will has smaller dynamic friction angle while smaller particle size will has larger
206 dynamic friction angle. The flow pattern of multi-size particle flow is more complicated compared
207 with the single size particle flow.

208 Figure 8 shows the flow pattern of multi-size particle flow. Segregation occurred when the
209 combined particles started flowing along the flume. Figure 8a demonstrates the flow pattern of
210 multi-size particle flow composing of white and black plastic balls. The diameter of the white
211 plastic ball is much larger than the black plastic ball as shown in Table 1. From the video captured
212 by the high speed camera, it is easy to observe that during the transportation period, white plastic
213 balls flowed on the upper layer while black plastic balls stayed at the bottom layer. This
214 phenomenon is consistent with the segregation theory of Savage et al. (1988). Besides, it is not
215 difficult to find that white plastic ball always stayed at the front of the flow where the velocity was
216 the highest, in other word, the velocities of the white plastic balls with relative larger diameters
217 are higher than the black plastic balls. Besides, at the upper layer where larger white plastic balls
218 are located, the inertial force dominated the flow dynamic and the energy dissipation was less than
219 that of the lower layer where the flow motion is mainly controlled by the contact forces. For the
220 forgoing reasons, it can be seen that large particle size leads to higher velocity during the flow.

221 Figure 8b shows the flow pattern of multi-size material composing of green glass balls and black
222 plastic balls. The diameter of green glass ball is similar to the diameter of black plastic ball, while
223 the density of green glass ball is almost two times larger than black plastic ball. In the upper
224 container, green glass balls were put statically at the top of the black plastic balls. After pulling up
225 the door, the black plastic balls flowed out firstly at the beginning and stayed at the bottom layer
226 due to the arrangement of the initial position of balls in the container, and then green glass balls
227 quickly moved downwards under the action of gravity, which leads to the fact that green glass
228 balls at the upper layer were replaced by black plastic balls subsequently. When the black plastic

229 balls form a stable contact network at the upper layer of the flow, the position transition or
230 segregation process stopped. In this case, the difference of particle sizes between two kinds of balls
231 is not obvious, and segregation was initiated due to the density difference only. During the
232 segregation process in which green glass balls moved downwards and black plastic balls migrated
233 upwards, the momentums of these two kinds of balls were transferred to each other at neighbor
234 location, therefore green glass balls and black plastic balls arrived at the catchment area almost at
235 the same time, while for the test in which balls were arranged in an opposite order (black plastic
236 balls at top and green glass balls at bottom), the green glass balls move faster and deposit earlier
237 at catchment area compared with the black plastic balls due to the smaller dynamic friction angle
238 as well as the larger kinetic energy of the green glass balls.

239 Similar to the above two figures, Figure 7c shows the flow pattern of transparent glass balls and
240 black plastic balls. In this case, both the density and particle size of the transparent glass balls are
241 larger than that of the black plastic balls. As shown in high speed camera video, during the flow
242 process, the transparent glass balls flow upwards and move faster in comparison with the black
243 plastic balls. Hence, although the density of the transparent glass balls is larger than the black
244 plastic balls, the transparent glass balls still stay at the upper layer of the granular flow due to their
245 relatively large particle sizes, which means that particle size has greater contribution for the
246 segregation process than density in the analysis of debris flow.

247
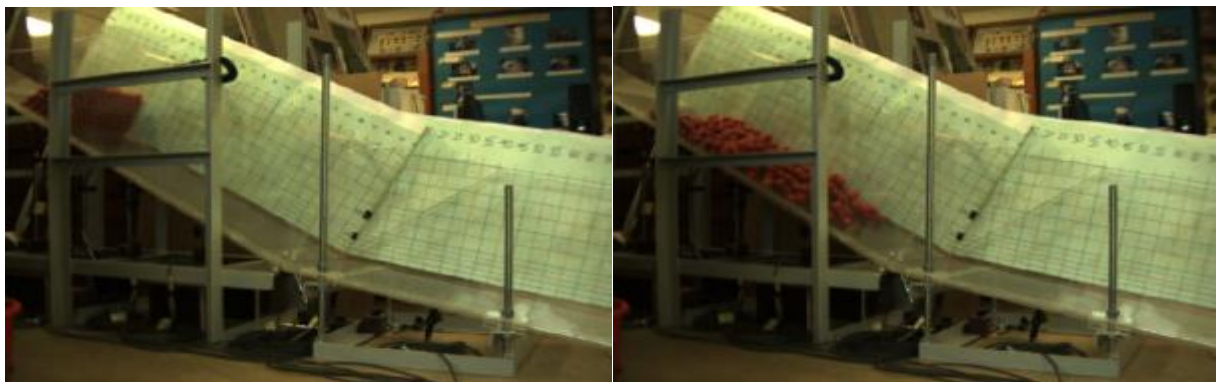
248

249

250 Fig. 7. Flow pattern of mono-size particle flow in physical model

251

252

253   a)   The influence of particle size on segregation process
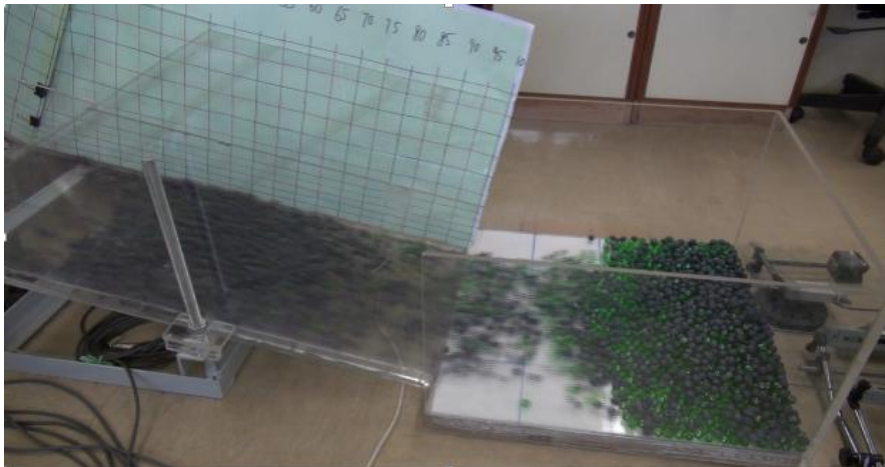
254

255   b)   The influence of density on segregation process

256

257   c)   The influence of particle size and density on the segregation process

258   Fig. 8. Flow pattern of multi-size particle flow

259

260   **3. Numerical Modeling of debris flow**

261   **3.1 Model generation**

262   Previous model tests by Chan (2001) for the runout were calibrated by the Dan model, where the
263   problem of segregation and flume jump were not considered. In general, the results are in
264   agreement with those from Rickenmann (in Jackobs and Hungr 2005). For the present studies
265   where multi-size particles are considered, the use of the simple Dan model is insufficient. The
266   laboratory tests in the present study are modelled using the distinct element method in this study,
267   which is more appropriate for the large deformation and separation phenomenon during the
268   transportation process. Once the appropriate numerical model is established, the numerical
269   technique will be extended to the field tests for which natural sand is adopted. In this paper
270   commercial program PFC2D using DEM has been adopted to implement the numerical simulation
271   of dry granular flow. Totally, there are five different methods of model generation in PFC2D
272   program, and based on the consideration time requirement, the rain method was adopted finally.
273   The parameters used in the numerical simulation are the micro-properties which are difficult to be
274   determined. Benchmark tests have been carried out in order to calibrate the micro-mechanical
275   properties of the dry granular material. Some of the micro-parameters of the balls are determined
276   through changing their values so that the macroscopic behaviors in numerical simulation are
277   consistent with that in physical test. The detailed micro-properties of the balls are shown in Table
278   3. Except for the wall friction (should be small as the walls are relatively smooth) and wall stiffness,
279   all the other parameters in Table 3 are determined by laboratory tests. In order to get different
280   frictional coefficients among the balls, two piece of wood which have plastic balls stick on it
281   regularly and shear force is applied. Furthermore, depositional tests, rebound tests are carried out
282   to measure the frictional angle and rebound coefficients of the balls. For each parameter, five
283   laboratory tests have been carried out, and the mean values are presented in Table 3. It should be
284   noted that there is not a wide distribution in the laboratory determined parameters, hence the range
285   of these parameters are not shown for clarity. The diameters of the particles in the numerical
286   analysis are the same as that used in the physical tests.

287

288   Table 3. Microscopic parameter of the balls for debris flow analysis

Balls	Ball stiffness (N/m^2)	Ball damp	Ball density (kg/m^3)	Ball friction	Wall friction	Wall stiffness (N/m^2)
Red plastic ball	2.36e9	0.4	1250	0.462	0.1	1.11e11

Black plastic ball	7e8	0.2	1250	0.1	0.1	1.11e11
Blue glass ball	7e10	0.3	2500	0.1	0.1	1.11e11
Green glass ball	7e10	0.2	2500	0.1	0.1	1.11e11

289

290

3.2 Numerical test results

A detailed comparison of the particle flow pattern modeled by the physical tests and discrete element analysis is shown in Figure 9. Figure 9a shows the physical test in which both the red plastic balls and green glass balls were used (too many test results are available, and only selected results are used for illustration in this paper). Large blue balls and small red balls in the numerical model represent the actual red plastic balls and green glass balls in the physical model tests respectively. A full-scale numerical simulation is rare to be conducted for discrete element analysis due to the limitation of the computer resource, but this is considered to be necessary and acceptable for the present study. Figure 9b shows the numerical results of the flow pattern of the multi-size particles. Particles start to flow along the flume after the initiation of the flow. During the flow process, the flow mass became longer under the action of shear force. Particles moved apart from each other and pushed other particles forwards. During this process, the momentums of the balls were exchanged and transferred to other balls at the neighbor locations. The flow velocity keep increasing until the front of the flow hit on the wall of the deposition zone. When the kinetic energy of the balls was exhausted, the balls eventually ceased to move at the catchment area. Figure 10 shows the flow pattern of multi-size balls flows composing of black plastic balls and green glass balls of which the diameter are relative smaller than the other balls as considered in the present paper. A pronounced Saltation was observed as balls flowed, implying that the collisional character of the flow mass where the savage number is larger than 0.1 (if the savage number is smaller than 0.1, the flow belongs to frictional flow, Iverson 1997). Savage number is the ratio between inertial force and frictional force. The comparison between Figure 10, and Figure 9b indicates that the larger the ball size, the more collisional the flow mechanism would be. As a result, the inertial forces dominate the flow dynamic compared with the frictional forces in the present tests. Furthermore, the balls at the upper region of the flow associated with higher velocity had more collisions and moved freely compared with that at the bottom region. The balls at the lower region were compacted with lower flow velocities. By comparison, the numerical simulation results of the flow pattern have a very good agreement with the physical test results when the micro-parameters were selected suitably.

As shown in Figure 9b and Figure 10, segregation was also observed in the numerical model after the dry granular balls started to move. In Figure 9b, it was evident that the blue balls with larger

321 ball size moved upwards and forwards, while the red balls with smaller ball size went to the lower
322 layer and stayed at the rear of the flow, which was consistent with the results in the physical model
323 tests. Smaller particles are more likely to move through the void between the larger particles, and
324 this will in turn squeeze the large particles to the upper layer of the flow. Because of the momentum
325 exchange between the balls and the flow mass dilation resulting from the shear deformation, a
326 dispersive pressure was caused which result in larger dry granular balls moved faster than the finer
327 particles and went upwards, and lead to the results that larger balls flowed to the upper layers
328 where the shear strain is low and accumulated at the front of the flow, while the finer balls tend to
329 moved downwards and accumulated at the bottom of the flow (Takahashi (1981)). Besides, the
330 difference of the ball size induce an unbalance forces on the balls which restrict the vertical
331 movement of the balls, and this will affects the flow segregation in the vertical direction. What's
332 more, the density difference between the balls the in numerical model is another factor that
333 influence the segregation process. Particles with lower density are more likely to rise to the free
334 surface while particles with higher density are more likely to segregate to the bottom of the flow.
335 From Figure 5b, it can be noticed that it is easily for the red balls with larger density traveled
336 through the gap generated by the shear deformation and squeezed the particle with smaller density
337 up to the upper flowing layer. The balls with higher density at the bottom pushed the balls with
338 smaller density forward. It is worth to mention that from the simulation results, the velocities of
339 the blue balls at free surface is the largest, which result in that the balls with large size migrated to
340 the front of the flow. The segregation mechanism simulated in the numerical model is in consistent
341 with what is aforementioned in the physical model tests. Ashwood and Hungr (2016), Choi et al.
342 (2014), Choi et al. (2015), Kwan (2012), Lo (2000), Ng et al. (2014), Ng et al. (2017) have
343 investigated the impact forces on the barrier which is however not investigated in the present study.

344

345

346

347

348

349

350
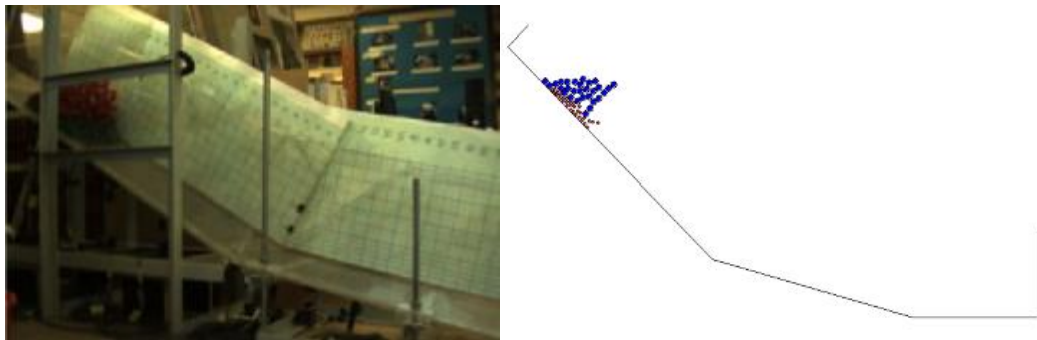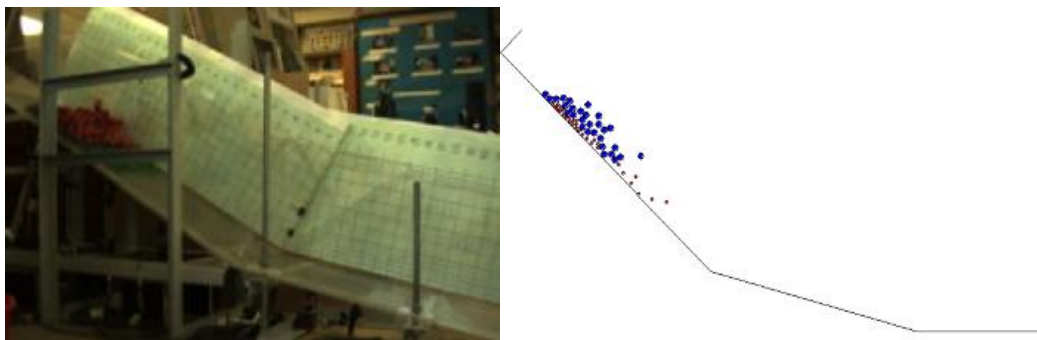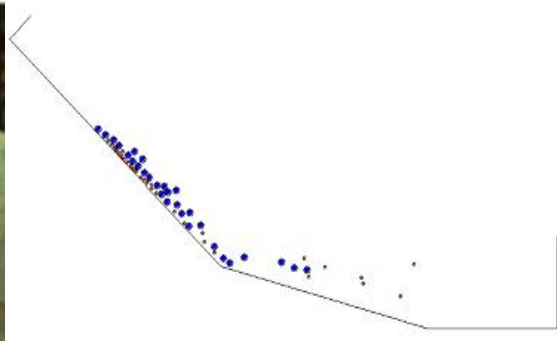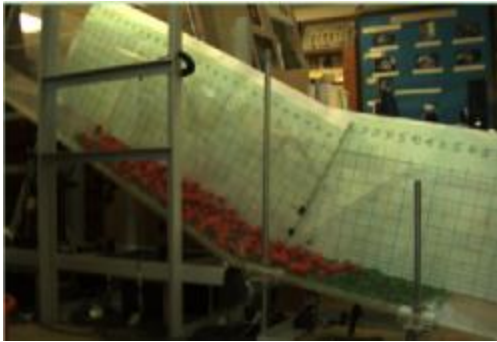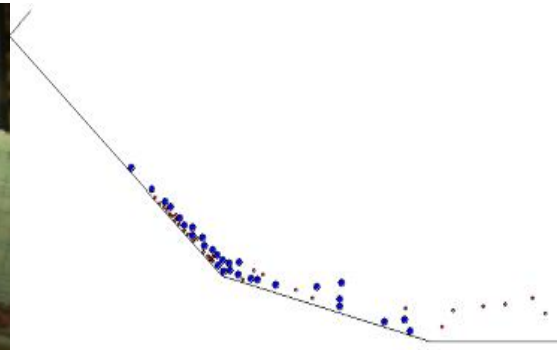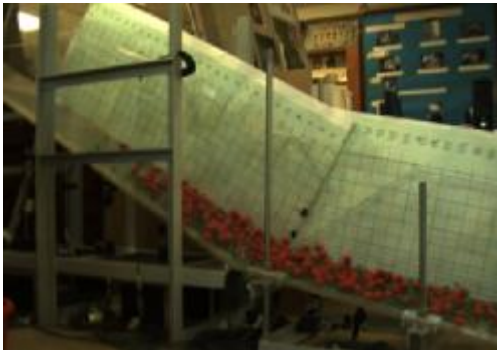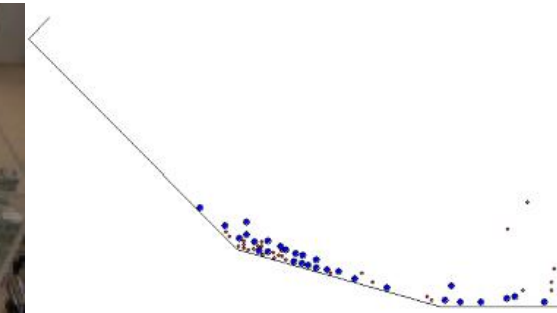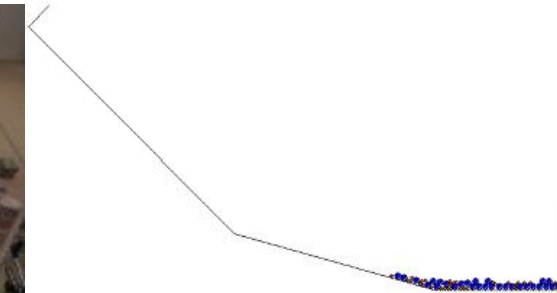
Fig. 9a. Flow pattern of multi-size   Fig. 9. Flow pattern of multi-size
          balls flow in physical test   balls flow in numerical test

Fig. 9. Flow Pattern of multi-size particle flow composing of red plastic balls and green glass
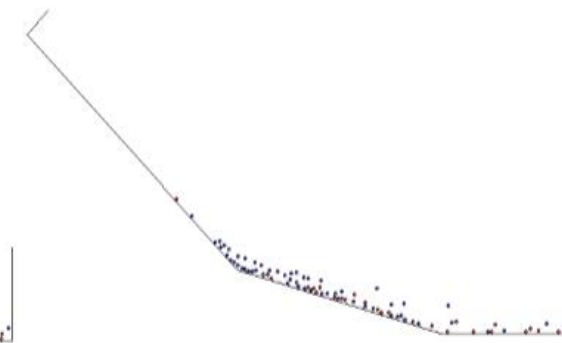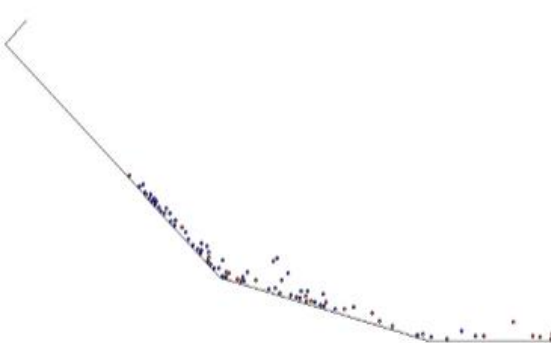   balls
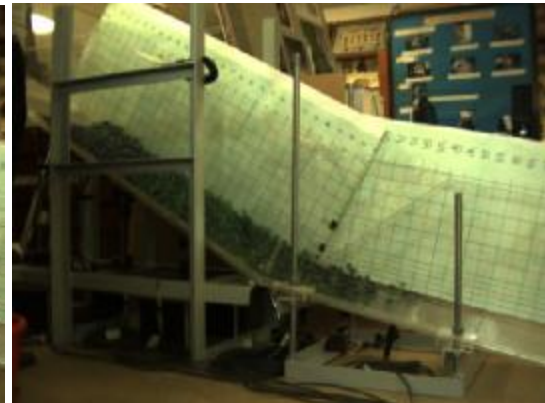
355

356
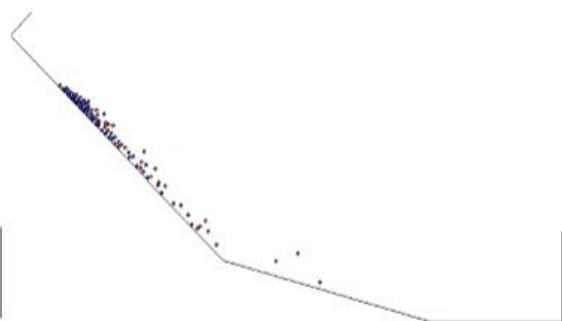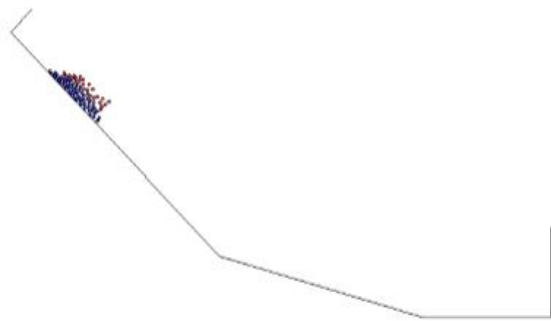
(a) Start of flow

(b) 1/3 of flow time
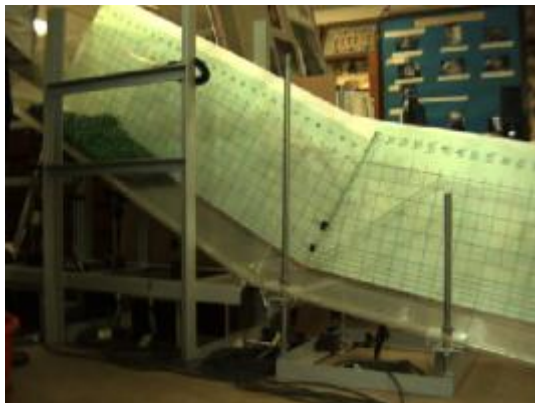
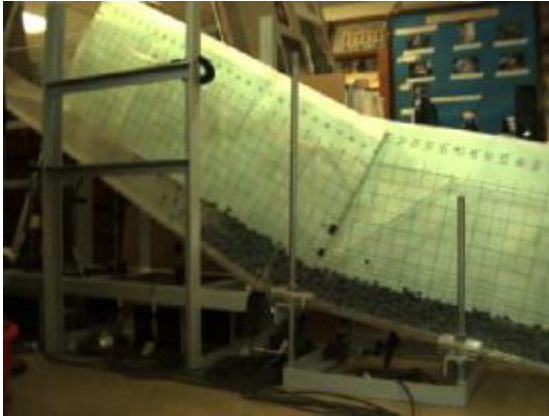357

358

(b) 2/3 of flow time

(d) end of flow

359

360

(e) Photo at start of flow

(f) photo at 1/3 of flow time

361
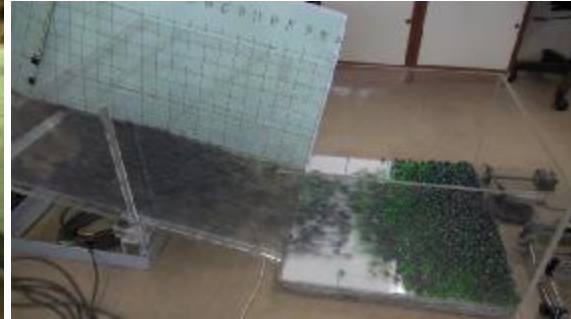
(g) photo at 2/3 of flow time   (h) photo at final stage

Figure 10. Flow Pattern of multi-size particle flow composing of black plastic

balls and green glass balls

3.3 The effect of the flume jump

Figure 11 shows the numerical results of the flow pattern of the blue glass balls flowing on the flume with or without a jump. The flow pattern of the blue glass balls flowing on the flume without a jump in the numerical model is almost the same as the flow pattern of the red plastic balls in the physical tests aforementioned. From the comparison of the flow pattern between Figure 11a and Figure 11b, an important phenomenon was observed. The run up height of the balls flowing on the flume with a jump is obviously lower than the run up height of the particles flowing on the flume without a jump, which indicates that flume jump is able to facilitate the process of energy attenuation and thereby has a good effect on suppressing the run up height of debris flow. This is also the reason why this jump is commonly adopted in Hong Kong for locations with potential small scale debris flow.

Figure 12 exhibits the velocity of the blue glass balls at different time step. In PFC2D, we have developed the code to monitor the maximum velocity of the balls for comparison purpose, and the monitored results are used to produce Fig.12. Black line represent the maximum velocity of the blue glass balls with 10Kg weight flowing on the flume without a jump at different time step, while the red line represent the same kind of balls with 13.55Kg weight on the flume with a jump. The comparison of the velocities at point A and point B indicates that the peak velocity of the balls flowing on the flume with a jump is pronouncedly smaller than that on the flume without a jump, and the peak speeds of the balls on the flume with a jump were achieved earlier than balls on the flume without a jump. It is worth to mention that the velocity of the balls is independent of the mass of the test material, except that at the peak period.

389 Figure 13 shows the velocity profile of mono-size particles (blue glass balls) along the flume with
390 or without a flume jump. The length of the velocity vector represents the speed of the particles.
391 From Figure 13, it can be noticed that the front flow velocities are the largest compared with the
392 velocities of the particles at the rear of the flow. When these particles approached the lower part
393 of the flume, the velocity directions changed due to the difference of the flume angles. This is in
394 good agreement with the laboratory results mentioned above. Figure 13b shows that the velocity
395 of mono-size particles on the flume with a jump increased after the initial state. The largest flow
396 velocity was achieved at the moment when these particles intend to jump into the deposition zone.
397 The directions of flow velocities changed and the speed of particles decrease as soon as they fell
398 into the deposition zone. As with those particles moving on the flume with a jump, the velocity of
399 the particles flowing along the flume without a jump increased when they approached the
400 deposition zone, however, the velocity of these particles kept increasing when they flowed into the
401 deposition area and the peak speed was achieved just before the moment when they reached the
402 boundary of the deposition area. When the granular front impacted on the wall of the deposition
403 area, these particles at the front of the flow reflect back and collide with the following particles,
404 and that is the moment when the flow speed decelerated.

405   According to Figure 12 and 13, the peak velocity of the balls on the flume with a jump achieved
406 before they impacted on the wall of deposition zone compared with that without a jump, which is
407 meaningful to the engineers because the flume jump can effectively reduce the impact force on the
408 barrier. Besides, the jump of the flume is capable of reducing the peak velocity of the dry granular
409 particle flow as well. To sum up flume jump, plays a vital role in attenuating debris flow, therefore,
410 flume jump is recommended to be applied in the design of debris flow barrier (which is actually
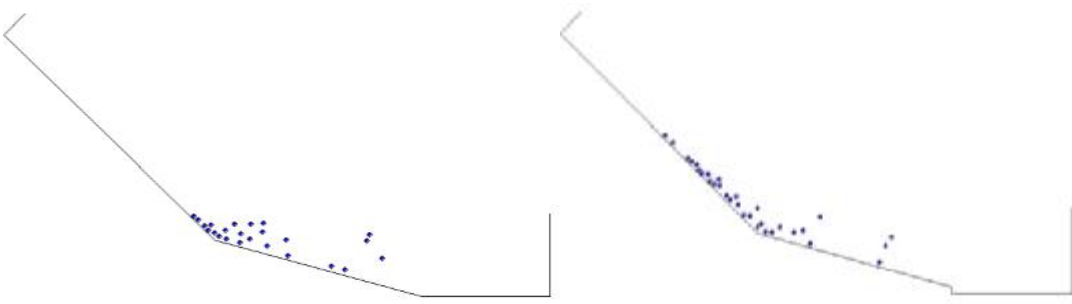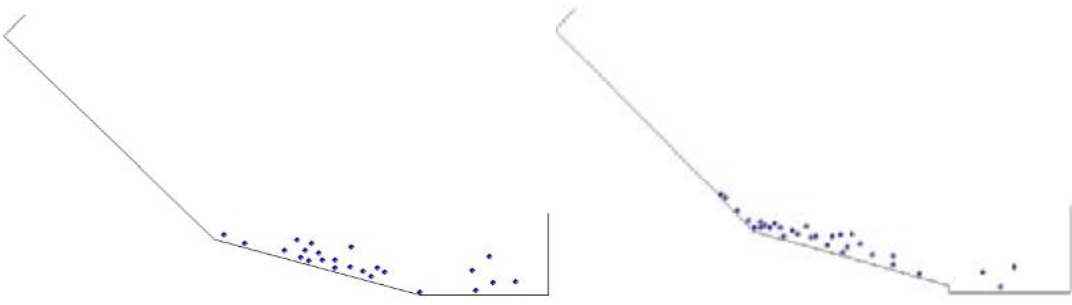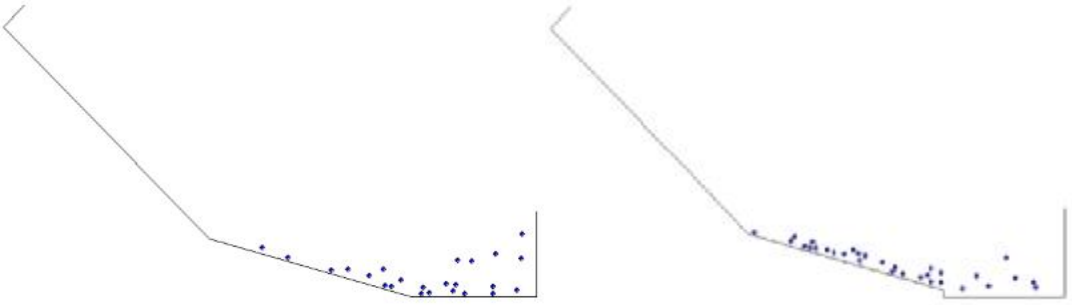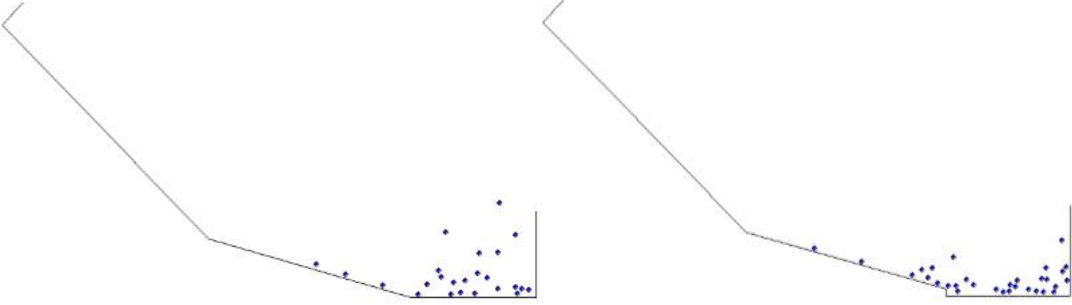411 adopted in Hong Kong and other places).

412

413

414
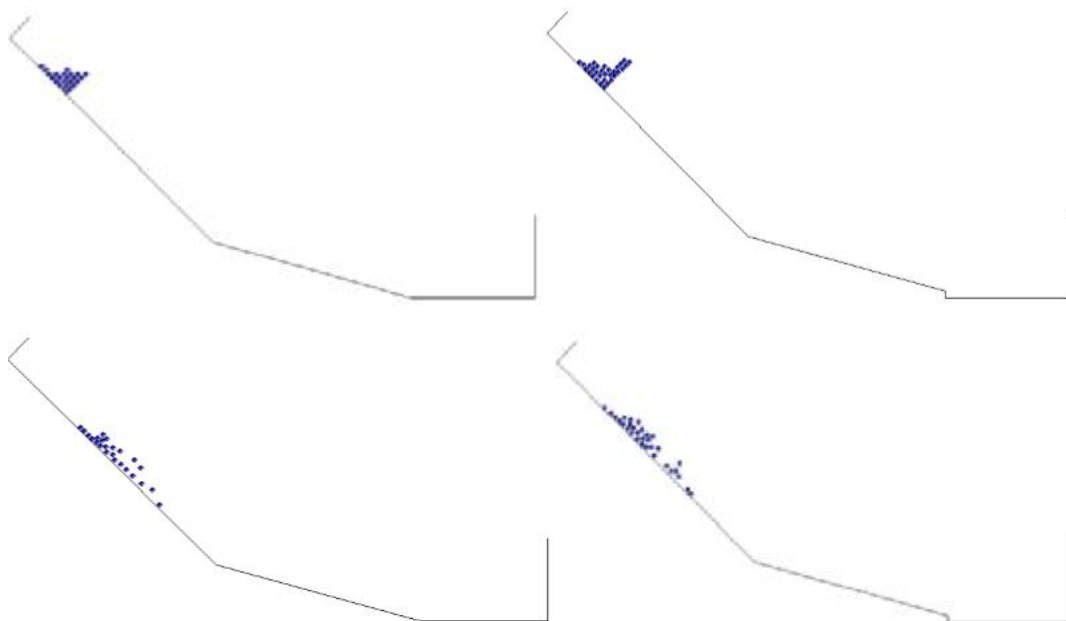
415

416

417

418

419
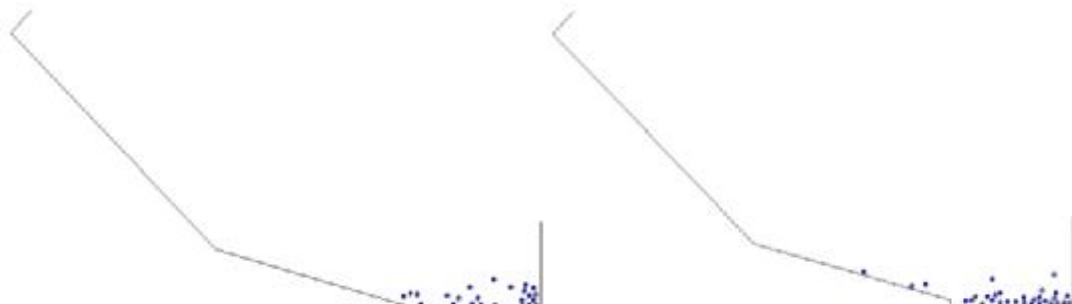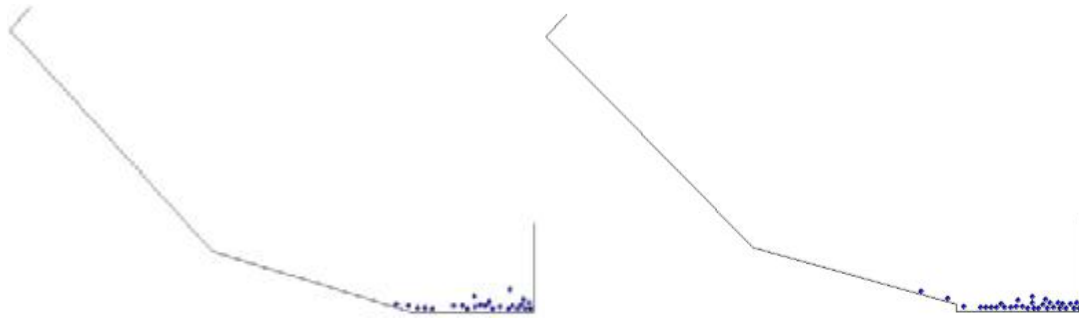
420

421 Fig. 11a. Flow pattern of blue glass balls   Fig. 11b. Flow pattern of blue glass balls

422 flowing along the flume without jump   flowing along the flume with jump

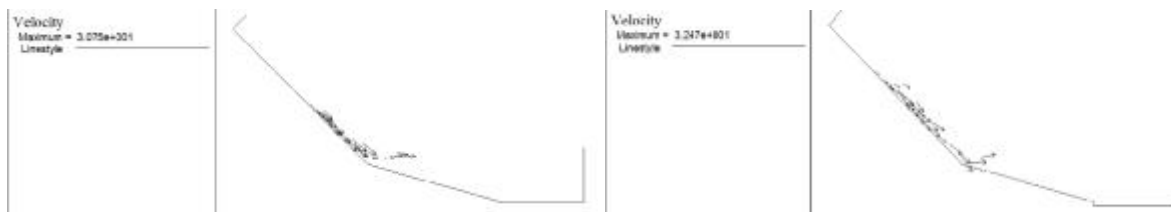423 Fig. 11. Flow pattern of blue glass balls flowing on the flume with or without a jump
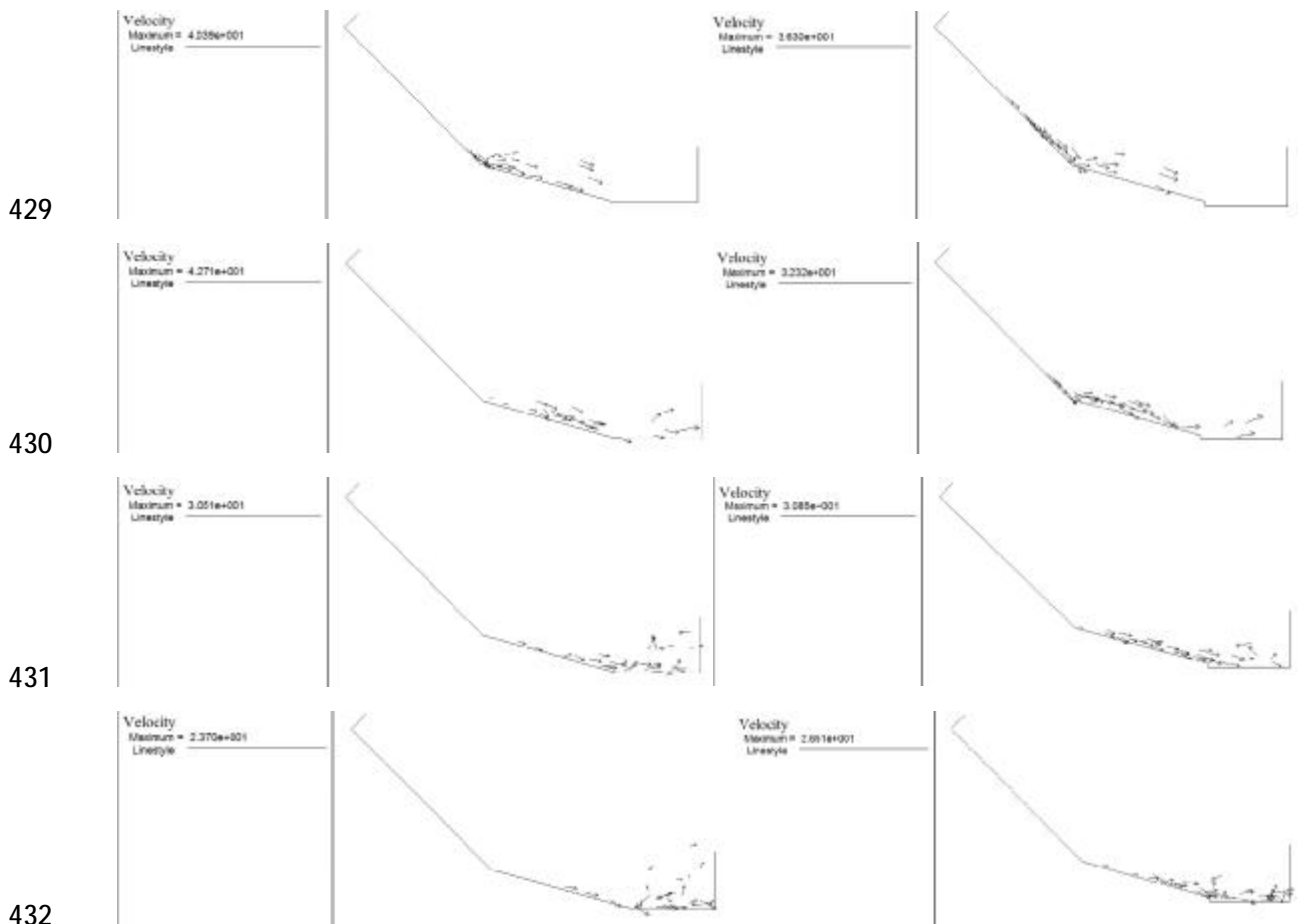
424
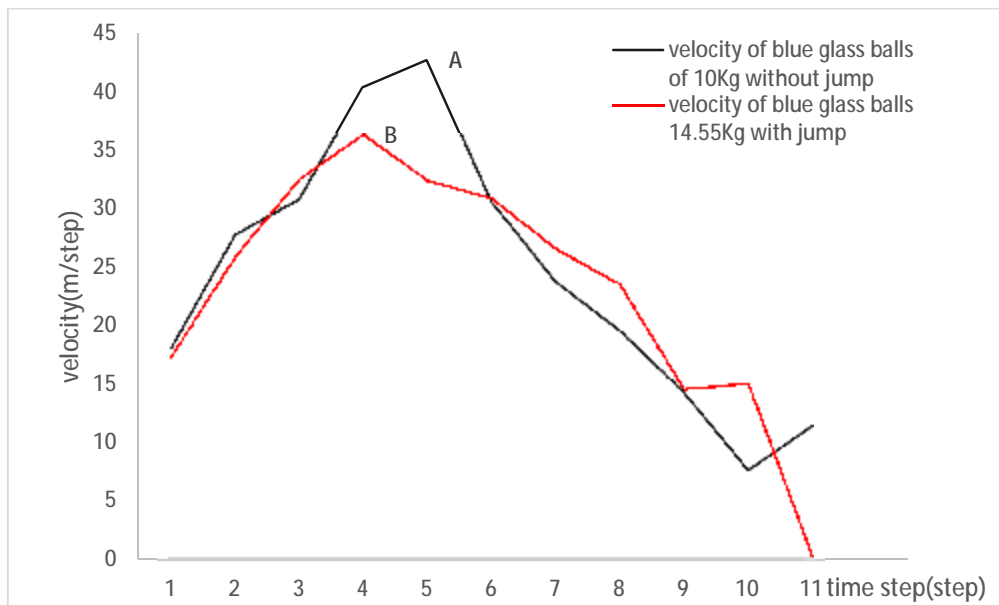
425

426 Fig. 12. Maximum velocity of blue glass balls in numerical model

427

428

429

430

431

432

Fig. 13a. Velocity profile of balls on the flume without a jump

Fig. 13b. Velocity profile of balls on the flume with jump

Fig. 13. Velocity profile of blue glass balls in numerical model

It should be that the actual flow velocity of the balls can be traced back from the high speed camera photos and the movie, but we do not present the results here because it is not the main theme of the present study. Most importantly, this is due to the limitations of DEM for which quantitative analysis is usually not good unless the micro-parameters are fine tuned. The authors do not prefer such tuning of the parameters, as such tuning cannot be performed the tests. However, the qualitative results from the DEM analysis and the laboratory tests are reasonable, hence we can still accept the results from DEM in our discussion. Actually, the authors have carried out limited tuning of the micro-parameters (not shown) in our internal studies. Since the flow and segregation process are practically not affected by the change of the parameters (but the actual value of the flow velocity, run-out … are affected), we have not included these results in the present paper, and the authors prefer to concentrate on the segregation and jump with a flume.

5. Large scale field tests

After the laboratory studies using a 1.5m long flume and glass/rubber balls, the authors have carried out a large scale flume test which is shown in Fig.14. The flume is about 6m long, and 5 types of sand as shown in Fig. 15 are used in the field tests. The particle size within each type is relatively uniform, and they ranged from 1-3mm, 3-5mm, 5-7mm, 7-8mm and above 8mm. The friction angles for the 5 types of sand as determined from the deposition tests as shown in Fig.15b are given by 28°, 30.3°, 29.1°, 31.5° and 33.7° respectively.

Fig.14 Large scale flume for field test

Fig.15a Sand used for debris flow tests   Fig.15b Deposition tests for sand

A series of tests with single, double and triple types of sand have been carried out, and only some of the results are shown in this paper for comparisons with the laboratory tests. As shown in Fig.16, the final deposition profile using type 1 (1-3mm) and type 4 (7-8mm) sands is shown. It is noticed that the coarse grain sand move to the top of the flow, which are illustrated by Fig.17a to 17c. Such results comply well with the laboratory studies. The control tests using coarse and finer sands are shown in Fig.18. A closer look into the difference between Fig. 18a and Fig.16 is the profile at the rear can reveal an important difference. For debris flow with 2 types of materials, the difference in the height of deposit for the first meter as measured from the left is greater than that for the test with single material (true for all single sand tests). Such phenomenon can be attributed to the effect

470 of the difference in the velocity flow between type 1 and 4 material, and type 1 material deposit at
471 the bottom during the flow. Based on the field tests, the importance of the particle size during the
472 segregation process as derived from the laboratory tests can be further verified.

473

474

475 Fig.16 Final deposition after the debris flow for two materials (coarse and fine)
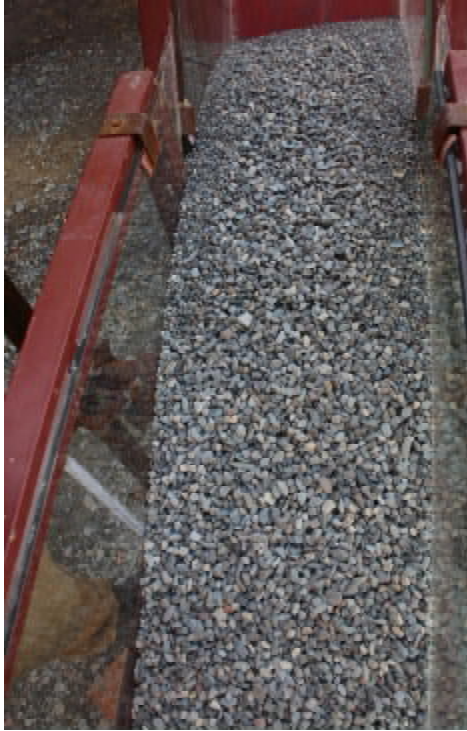

476

477 Fig.17 a Deposition at the rear of the deposit   Fig.17b Deposition at the front of the deposit

478

479

Fig.17c Front view of the deposition (2 materials)

481

482

Fig.18a Front view of the deposition (type 4 material) Fig.18b Close up view of the deposition

484

With reference to Fig.19, it is clear that the formation of the flow front, flow head, channelized flow and levee from the present field test is very similar to that by Johnson et al. (2012). The surface trajectories of the particles by Johnson et al. (2012) are also captured by the high speed camera in the present laboratory and field tests. A coarse enriched surface layer has been obtained by Johnson et al. (2012), and such phenomena are also obtained from the laboratory and field tests and is clearly illustrated in Fig.17. Iverson (1997) has also found similar segregation from the

491   debris flow at Oregon (1996). It should be noted that for all the debris flow tests in the present
492   study, such segregation phenomenon is always obtained, as long as there are more than 1 materials
493   in the problems.

494

495   Fig.19 Front of the runout

496   **6. Discussion**

497   Laboratory tests were carried with numerical simulations through distinct element method to study
498   the flow pattern of dry granular flow. The study is important for the basic understanding of the
499   debris flow segregation problem and the importance of providing a jump in the flume or in the
500   actual protective measures. For the present tests, the flume base is even and smooth which result
501   in relative small dynamic frictional angle and less energy attenuation compared with the debris
502   flow. Besides, the surfaces of the glass and plastic balls used in the experiments are regular and
503   smooth, while for debris flow occurring in nature the debris materials are irregular and rough,
504   which cause the dynamic internal frictional shear force between real scale debris flow particles are
505   relatively large and hence the run up height is lower. As a consequence, it is a conservative method
506   of present tests to study the flow pattern of debris flow. Such arrangement is necessary so as to
507   clearly identify the contribution of particle size distribution in the segregation process.

508

509   Physical tests were conducted to study the flow pattern of mono as well as multiple size particle
510   flows. In general, the results from the present study comply well with those from the literature.
511   Test results indicate that flow mass elongated under the action of shear force during the particles
512   flowed on the flume. For multi-size particles with different particle sizes, segregation always
513   occurs. Particles with larger diameters migrated upward and small particles moved downwards
514   because particles with smaller diameter can go through the gap between the larger particles. In

515   addition, the density of the particle is another factor that play a role in the segregation process.
516   Under the action of gravity, particles with higher density moved downwards faster and other
517   particles with lower density were squeezed up. For the real scale debris flow, the debris material
518   ranges from clay and silt to boulders while the differences in the densities between different types
519   of particles are relatively small, hence particles size will be the most dominant factor which
520   influence the segregation process. Top view from the high speed camera indicates that the
521   velocities of the large particles are higher than the velocities of the small particles. Granular
522   particles with larger particles sizes travelled to the front of the flow where the velocities are higher.
523   Larger particle size is observed to lead to a higher velocity. Such results are also in general
524   agreement with the results by Takahashi (1980).

525   For the flow pattern of dry granular particles simulated through distinct element method, the
526   simulation results of flow pattern are almost the same as the physical tests. Berger (2016), Chen
527   and Lee (2000), Ghilardi et al. (2001) also obtained a reasonably well numerical modeling of the
528   flow process for relatively simple flow problem which support the use of numerical analysis for
529   the debris flow problem. In the present numerical model, a pronounced segregation process was
530   observed as well, which comply well with many previous studies by Gray et al. (2003),
531   Hákonardóttir et al. (2003), Iverson (1997), Johnson et al. (2012) and many others. Large particles
532   went upwards while small particles went downwards. From the velocity vector figure, the
533   velocities of the particles at upper layer as well as the velocities at the front of the flow were the
534   largest. Savage numbers of the dry granular particles in present tests were larger than 0.1, which
535   represent the collisional character of the flow. The flow behavior was hence more inertial than
536   frictional. Flume jump have a significant influence on the impeding debris flow. When the particles
537   flowed through the jump a large quantity of kinetic energy were consumed during this process.
538   The peak velocities of particles flowing on the flume with a jump were lower than that without a
539   flume jump. Besides, the peak velocities of the particles on the flume with a jump were achieved
540   earlier, and after that the flow velocity started to decrease, which would make a great contribution
541   for reducing the impact load. The run up height of the particles on the flume with a jump was
542   apparently lower than that without a jump. Thus, flume jump can help to reduce the flow velocity
543   as well as suppress the run up height.

544   Comparing the physical and numerical test results, the macroscopic flow behavior in numerical
545   models are consistent with the physical tests. Through a good selection of the model generation
546   method and micro parameters, the distinct element method can produce a reasonable qualitative
547   simulation of the behavior of dry granular flow for the consideration of the engineers. These results
548   have useful contributions to the better understanding of the debris flow behavior which is not
549   possible for other classical methods. Up to the present, the engineers are still relying on some
550   empirical methods such as dynamic impact earth pressure coefficient (Kwan 2012) or similar
551   approaches for the design of flexible or rigid barrier, as debris flow process is complicated by
552   many geotechnical and geographical complexities. The design of the barrier is still more an art
553   than science up to the present, though some guidelines are available to help the engineers in the
554   design. Distinct element analysis is well known to be more suitable for qualitative than quantitative
555   description. It is possible to tune the parameters so as to give quantitative matching, but this is not
556   the purpose of the present work. Without test measurement, such matching is not possible. The

purpose of the present work is to demonstrate the general applicability of the distinct element modelling in dry granular flow problem. For the tuning of the parameters to give quantitative comparisons, this is trivial and will not be discussed here, as this is not the main theme of the present work. So far, quantitative study using DEM is still difficult, due to various difficulties in micro-parameters determination, contact model and other factors. These limitations are well known, and up to now are still open questions. The focus of the present paper is the segregation process from a qualitatively assessment, and the authors are also working on the possibility of quantitative DEM assessment so as to compare the computed results with the actual laboratory and field tests results on velocity of parameters and other information. However, the DEM analysis in this study is used to supplement the field and laboratory studies instead being the main theme of the present work, hence no detailed comparisons between the results from tests and DEM analysis is carried out. Some tuning of the micro-parameters have been carried out (not shown), but the overall behavior is practically not affected, as the segregation process is largely controlled by the particle size.

The flow process and segregation process from laboratory and field tests are similar in many respect – largely controlled by the particle size distribution. This is clearly illustrated from about 50 tests in our study. Limited photos are shown in this paper to limit the length of the paper. Thousands of photos and about a hundred movie files are obtained from the laboratory and field tests in this study, and only selected photos which are sufficient to illustrate the main purposes of the present work are shown in the present paper. The authors are however happy to share these materials upon request at ceymchen@polyu.edu.hk.

7. Conclusion

In the present study, two important phenomena in debris flow are studied. The first problem is the segregation process which is captured in all the tests in the present studies. The segregation phenomenon can affect the design of the barrier in different ways. The finer materials will be deposited at the bottom of the runout, and the relatively lower permeability of this layer will tend to drive the water level upward (somewhat similar to the perch water table phenomenon). This may increase the destructive power of water. For the design of rigid barrier, the use of a suitable water table will also be crucial to maintain adequate factor of safety of the barrier. Since segregation will occur practically for majority of the debris flow problems, this effect should be well studied and considered in the design of flexible and rigid barriers.

The authors have chosen flexible spherical rubber beads as well as rigid glass beads for the laboratory, and the range of stiffness would be sufficient to cover most of the natural flow materials. The segregation process as found from the laboratory test is actually similar to that in the field tests using non-spherical sand. Through such selection, it is clearly demonstrated that particle size

distribution is a very critical factor in the segregation process, and it appears that it is more critical than particle shape or stiffness.

To reduce the destructive power of the debris, a small jump in the flow channel is sometimes applied in Hong Kong if the site condition allow. In general, the effect of this jump is small, and is effective only for small volume debris flow which is the common case for Hong Kong. Nevertheless, such provision can slightly reduce the destructive power of the debris. It is interesting to note that there is virtually no study about the effect of the jump in the past, and the present work provide some useful pilot works, for which more works may come out in the future.

The authors are currently considering the next stage of field tests, for which the wet test will be carried out, and more equipment and measurements will also be used. There are however some practical considerations which include time, money, and the setup of the test materials and other factors. Currently, the authors are constructing a laboratory flume where the base is rough. The combined effect of base roughness and flume inclination angle will be carried out soon, and hopefully the results will form the extension of the present paper. For the field test, most of the researchers place a contained of wet sample and let the sample flow down. This approach is simple to be executed, but the actual debris flow may not be like that. From the observations of several debris flows in Hong Kong, the authors have noticed that erosion process is an important phenomenon in Hong Kong which is not simple to be reproduced in the field flume. The composition of the flow material actually changes during the flow process. More thoughts will be given to the setup of the wet field test in the future, and the base of the flume may be specially prepared with some soil bedding to allow for erosion in the future tests.

Reference

Ashwood, W., & Hungr, O. (2016). Estimating total resisting force in flexible barrier impacted by a granular avalanche using physical and numerical modeling. Canadian Geotechnical Journal, 53(10), 1700-1717.

Berger C. (2016), A comparison of physical and computer-based debris flow modelling of a deflection structure at Illgraben, Switzerland, INTERPRAEVENT 2016, 212-220.

632 Chan, C. P. L. (2001). Runout distance of debris flows: experimental and numerical simulations
633 (Doctoral dissertation, The Hong Kong Polytechnic University).

634 Chen H. and Lee C.F. (2000), Numerical simulation of debris flow, Canadian Geotechnical
635 Journal, 37:146-160.

636 Cheng Y.M., Liu H.T. and Au S.K. (2005), Location of critical three-dimensional non-spherical
637 failure surface with applications to highway slopes, Computers and Geotechnics, no. 32, 387-399.

638 Cheng YM, Li N. and Yang XQ (2015), Three Dimensional Slope Stability Problem with a
639 Surcharge Load, Natural Hazards And Earth System Sciences, 15(10), 2227-2240.

640 Choi, C. E., Au-Yeung, S. C. H., Ng, C. W., & Song, D. (2015). Flume investigation of landslide
641 granular debris and water runup mechanisms. Géotechnique Letters, 5(1), 28-32.

642 Choi, C. E., Ng, C. W., Song, D., Kwan, J. H. S., Shiu, H. Y. K., Ho, K. K. S., & Koo, R. C. H.
643 (2014). Flume investigation of landslide debris–resisting baffles. Canadian Geotechnical Journal,
644 51(5), 540-553.

645 Coussot, P. and Meunier, M, (1996), Recognition, classification and mechanical description of
646 debris flows, Earth-Science Reviews, 40: 209–227.

647 Cruden,D.M. and Varnes, D.J., (1996), Landslide Types and Processes, Special Report ,
648 Transportation Research Board, National Academy of Sciences, 247:36-75

649 Cundall, P. A. (1971). A computer model for simulating progressive large scale movements in
650 blocky rock systems. In Proc. Symp. Rock Fracture (ISRM), Nancy, France, 129-136.

651 Cundall P A. (1988), Formulation of a three-dimensional distinct element model—Part I. A
652 scheme to detect and represent contacts in a system composed of many polyhedral blocks,
653 International Journal of Rock Mechanics and Mining Sciences & Geomechanics Abstracts.
654 Pergamon, 25(3): 107-116.

655 Cundall, P. A. and Hart, R. D. (1992). Numerical modelling of discontinua. Engineering
656 Computations, 9(2), 101-113.

657 Cundall, P. A. and Strack, O. D. (1979). A discrete numerical model for granular assemblies.
658 Geotechnique, 29(1), 47-65.

659 Furuya, T., 1980, Landslides and landforms: in Landslides, slope failures and debris flows

660 (Takei, A. ed.), Kajima Shuppan, Tokyo, pp.192–230.

661 Ghilardi P., Natale L. and Savi F. (2001), Modeling debris flow propagation and deposition,
662 Phys. Che. Earth 9:951-656.

663 Gray, J. M. N. T., Tai, Y. C., & Noelle, S. (2003). Shock waves, dead zones and particle-free
664 regions in rapid granular free-surface flows. Journal of Fluid Mechanics, 491, 161-181.

665 Hákonardóttir, K. M., Hogg, A. J., Batey, J., & Woods, A. W. (2003). Flying avalanches.
666 Geophysical Research Letters, 30(23).

667   Halsey and Mahta (2002), Challenges in Granular Physics, World Scientific

668   Hungr, O. (1995), A model for the runout analysis of rapid flow slides, debris flows, and
669   avalanches, Can. Geotech. J., 32, 610–623.

670   Hungr O., Evans S.G., Bovis M. and Hutchinson J.N. (2001), Review of the classification of
671   landslides of the flow type, Environmental and Engineering Geoscience, VII, 221-238.

672   Hutter, K., Wang, Y., & Pudasaini, S. P. (2005). The Savage–Hutter avalanche model: how far
673   can it be pushed? Philosophical Transactions of the Royal Society of London A: Mathematical,
674   Physical and Engineering Sciences, 363(1832), 1507-1528.

675   Iverson, R. M., Reid, M. E., & LaHusen, R. G. (1997). Debris-flow mobilization from landslides
676   1. Annual Review of Earth and Planetary Sciences, 25(1), 85-138.

677   Iverson, R. M., & LaHusen, R. G. (1989). Dynamic pore-pressure fluctuations in rapidly
678   shearing granular materials. Science, 246(4931), 796-800.

679   Iverson, R. M., & LaHusen, R. G. (1993). Friction in debris flows: Inferences from large-scale
680   flume experiments. American Society of Civil Engineers (Ed.), Hydraulic Engineering, 93.

681   Iverson R.M. (1997), The physics of debris flows, Reviews of Geophysics, 35(3):245-296.

682   Iverson, R.M., and George, D.L., (2016), Discussion of "The relation between dilatancy,
683   effective stress and dispersive pressure in granular avalanches" by P. Bartelt and O. Buser, Acta
684   Geotechnica, 11(6), 1465-1468

685   Jackob M. and Hungr O. (2005), Debris flow hazards and related phenomena, Springer Praxis.

686   Jiang, M., J. Konrad, and S. Leroueil (2003). An efficient technique for generating homogeneous
687   specimens for DEM studies, Computers and Geotechnics 30, 579–597.

688   Johnson A.M. (1996), A model for grain flow and debris flow, U.S. Department of the Interior
689   U.S. Geological Survey, Open-file-report 96-728.

690   Johnson C.G., Kokelaar B.P., Iverson R.M., Logan M., LaHusen R.G. and Gray J.M.N.T.
691   (2012), Grain-size segregation and levee formation in geophysical mass flows, Journal of
692   Geophysical Research, 117, F01032.

693   Kesseli, J. E. (1943). Disintegrating soil slips of the Coast Ranges of Central California. The
694   Journal of Geology, 51(5), 342-352.

695   Scott K. M. and Wang Y.Y. (1997), Debris flow - Geological process and hazard illustrated by a
696   surge sequence at Jiangjia ravine, Yunnan, China, U.S. Geological Survey Professional Paper
697   1671.

698   King J.P. (2013), Tsing Shan Debris Flow and Debris Flood, GEO Report No. 281, Hong Kong
699   SAR Government.

700 Kwan, J. S. H. (2012). Supplementary technical guidance on design of rigid debris-resisting
701 barriers. Geotechnical Engineering Office, HKSAR. GEO Report, (270).

702 Li K.H. (2013), Laboratory debris flow flume test, Hong Kong Polytechnic University.

703 Lin, D. G., Hsu, S. Y., & Chang, K. T. (2009). Numerical simulations of flow motion and
704 deposition characteristics of granular debris flows. Natural hazards, 50(3), 623-650.

705 Liu, X. (1996). Size of a debris flow deposition: model experiment approach. Environmental
706 Geology, 28(2), 70-77.

707 Lo, D. O. K. (2000). Review of natural terrain landslide debris resisting barrier design. HKSAR:
708 GEO, Report no. 104.

709 Lo, K. H. (2004). Theoretical simulations of debris flow and their applications to hazard
710 mapping using GIS (Doctoral dissertation, The Hong Kong Polytechnic University).

711 Lo O.K., Law H.C., Wai C.T., K.L. Ng, Williamson S.J., Lee K.S. and Cheng Y.M. (2018),
712 Investigation of an unusual landslide at Sai Kung Sai Wan Road, Sai Kung, HKIE Transaction
713 Theme issue on landslides and debris flow, 102-114.

714 Major, J. J. (1997). Depositional processes in large-scale debris-flow experiments. The Journal
715 of Geology, 105(3), 345-366.

716 Mancarella D. and Hungr O. (2010), Analysis of run-up of granular avalanches against steep,
717 adverse slopes and protective barriers, Canadian Geotechnical Journal, 2010, 47(8): 827-841

718 McDougall and Hungr (2004), A model for the analysis of rapid landslide motion across three-
719 dimensional terrain, Canadian Geotechnical Journal, 41(6): 1084-1097

720 Mizuyama, T., Uehara.S., (1983), Experimental study of the depositional process of debris flows.
721 Trans. Jpn. Geomorph. Union 4, 39-64.

722 Ng, C. W. W., Choi, C. E., Kwan, J. S. H., Koo, R. C. H., Shiu, H. Y. K., & Ho, K. K. S. (2014).
723 Effects of baffle transverse blockage on landslide debris impedance. Procedia Earth and
724 Planetary Science, 9, 3-13.

725 Ng, C. W. W., Choi, C. E., Liu, L. H. D., Wang, Y., Song, D., & Yang, N. (2017). Influence of
726 particle size on the mechanism of dry granular run-up on a rigid barrier. Géotechnique Letters,
727 7(1), 79-89.

728 Ohyagi, N., 1985, Definition and classification of sediment hazards: in Prediction and
729 countermeasures of sediment hazards (Japanese Soc.Soil Mech. Foundation Eng. ed.), Japanese
730 Soc. Soil Mech. Foundation Eng., Tokyo: 5–15.

731 Pierson, T.C. and Costa, J.E., 1987, A rheologic classification of subaerial sediment-water flows:
732 in Debris flows/avalanches: process, recognition, and mitigation (Costa, J.E. and Wieczorek,
733 G.F. eds.), Rev. Eng. Geol., 7, Geolo. Soc. Am: 1–12.

734 Pudasaini S.P., Wang Y. and Hutter K. (2005), Modelling debris flows down general channels,
735 Natural Hazards And Earth System Sciences, 5, 799-819.

736 Pudasaini & Hutter (2007), Avalanche Dynamics, Dynamics of Rapid Flows of Dense Granular
737 Avalanches, Springer Verlag.

738 Rodine, J. D., Johnson, A. M., & Rich, E. I. (1974). Analysis of the mobilization of debris flows.
739 STANFORD UNIV CALIF DEPT OF GEOLOGY.

740 Rodolfo, K. S., Umbal, J. V., Alonso, R. A., Remotigue, C. T., Paladio-Melosantos, M. L.,
741 Salvador, J. H. and Miller, Y. (1996). Two years of lahars on the western flank of Mount
742 Pinatubo: Initiation, flow processes, deposits, and attendant geomorphic and hydraulic changes.
743 Fire and mud: eruptions and lahars of Mount Pinatubo, Philippines, 989-1013.

744 Mizuyama, T., & Uehara, S. (1983). Experimental study of the depositional process of debris
745 flows. Japanese Geomorphological Union, 4(1), 49-63.

746 Savage, S. B. and Hutter, K. (1989), The motion of a finite mass of granular material down a
747 rough incline, J. Fluid Mech., 199, 177–215.

748 Savage S.B. and Lun C.K.K. (1988), Particle size segregation in inclined chute flow of dry
749 cohesionless granular soils, J. Fluid Mech., 199, 177-215.

750 Sullivan, C. (2011). Particulate discrete element modelling. Taylor & Francis.

751 Takahashi, T. (1981). Debris flow. Annual review of fluid mechanics, 13(1), 57-77.

752 Takahashi, T., (2001), Mechanics and simulation of snow avalanches, pyroclastic flows and
753 debris flows, Spec. Publs., Int. Ass. Sediment, 31: 11–43.

754 Takahashi, T., (2006), Mechanisms of sediment runoff and countermeasures for sediment
755 hazards, Kinmirai Sha.

756 Takahashi T. (2014), Debris Flow - Mechanics, Prediction and Countermeasures, 2nd edition,
757 CRC Press.

758 Varnes, D.J., (1978), Slope movement types and processes: in Landslides analysis and control
759 (Scguster, R.L and Krizek, R.J. eds.), NAS Sp. Rep. 176: 11–33.

760 Voellmy, A. (1955), Über die Zerstörungskraft von Lawinen. Schweizerische Bauzeitung 73,

761 159–162, 212–217, 246–249, 280–285. In German.

762 Yamashiki Y., Mohd Remy Rozainy M.A.Z.c, Matsumotod T., Takahashie T. and Takarabc K.
763 (2013), Particle Routing Segregation of Debris Flow Mechanisms Near the Erodible Bed,
764 Procedia APCBEE, 527-534.

765 Zohdi, T. I. (2007), P-wave induced energy and damage distribution in agglomerated granules
766 Modelling and simulation in materials science and engineering. 15, S435-S448.

767   Zhou G.D., Law R.P.H. & Ng C.W.W. (2009), The mechanisms of debris flow: a preliminary
768   study, Proceedings of the 17th International Conference on Soil Mechanics and Geotechnical
769   Engineering, 1570-1573.